Application of intelligent materials to enhance SPAR floating offshore platforms stability

Maria Rius Planas

Dept. Mechanical Engineering, Instituto Superior Técnico, Universidade Técnica de Lisboa

Lisbon, Portugal

ABSTRACT

The following article resumes the results obtained from a stability study of a floating wind turbine spar platform, composed of two concentric cylinders, for offshore application. Optimum dimensions are calculated minimizing the vertical forces, formulated with linear wave theory simplifications. An inertial plate is added to stabilize the platform for a large frequency bandwidth due to the increment of the added mass coefficient and the consequent reduction of the resonance frequency. The porosity of the inertial plate affects the resonance frequency and can be adapted to the incident wave frequency to reduce the high motions of the spar. The corrosion problems of the offshore platforms are studied in order to choose an appropriate material for the spar components. Finally, a mechanical system is designed to simulate the porosity variation of the inertial plate.

KEY-WORDS: Wind offshore energy; stability; linear theory; inertial plate; porosity control; corrosion.

INTRODUCTION

During the last years many European countries have been investigating and developing systems for obtaining energy in the sea. On a national level, the Wave Energy Centre (WaveEC) was founded in 2003 and is collaborating with Portuguese and international companies doing R&D and developing projects in all kinds of sea technologies.

Offshore wind turbines are being used in a number of countries to harness the energy of the moving air over the oceans and convert it to electricity. Offshore winds tend to flow at higher speeds than onshore winds, thus allowing turbines to produce more electricity. Moreover, they help to reduce impacts on human activities and ecosystems, [7].

The first offshore floating wind platform is nowadays becoming operational in Portugal. The country is participating in a project with the support of the American company Principle Power technology and EDP. The project involves the construction of a 2 MW wind turbine prototype during the autumn of 2011.

The support structure of floating offshore wind turbines should be as most stable as possible for a wide range of frequencies. Depending on the frequency of the incident wave the spar stability can be affected significantly, especially close to the resonance frequency. The present project concerns the use of smart materials or other equivalent solutions to change the shape of floating structures so that they become more stable under different wave periods. Nowadays, the use of smart materials in that application is an open field, which increases the difficulty in the search of the best solution. In this context, the Centre for nanotechnology and Smart Materials, (CeNTi) has collaborated with the present project.

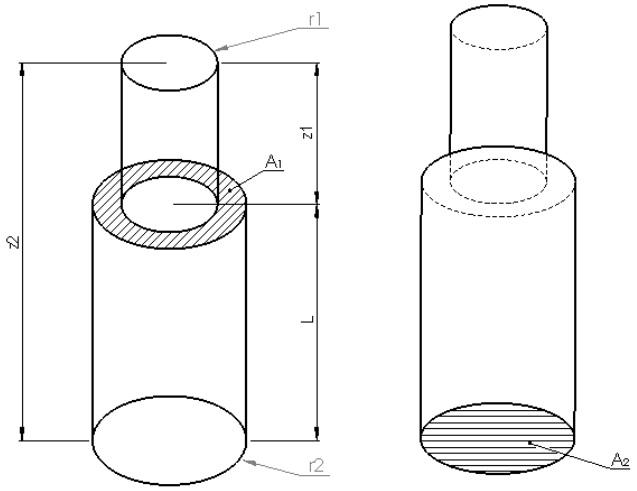

Fig. 1: Schematic representations of the spar structure with the variables of study.

DYNAMICS OF A SPAR BUOY

Assumptions

The SPAR will be floating in the sea and supporting the windmill. Some assumptions should be accepted henceforth to create a model of the body.

Here it is assumed that the fluid is inviscid allowing the Euler equations to apply. Moreover, the mass must be conserved. The mathematical equation in two dimensions to express the assumption that water is incompressible (ρ constant $\rightarrow \nabla \cdot \mathbf{v} = 0$) is given by the following form of the continuity equation (1):

$$\frac{\partial u}{\partial x} + \frac{\partial w}{\partial z} = 0 \tag{1}$$

Where *u* is the *x* direction velocity and *w* is the *z* direction velocity, *x* is the horizontal direction and *z* is the vertical rising direction which is *0* in the middle position of the free surface. Water will be assumed as an inviscid and incompressible fluid. Thus, there are only normal stresses (pressures) acting on the surface of a fluid particle; since the shear stresses are zero, there are no stresses to impart a rotation on a fluid particle. Therefore, the motion is irrotational.

The Bernoulli equation provides a relationship between the pressure field and kinematics. The resulting equation is:

$$-\frac{\partial \emptyset}{\partial t} + \frac{1}{2}(u^2 + w^2) + \frac{p}{\rho} + gz = C(t) \tag{2}$$

Where $\emptyset$ is the velocity potential, *t* is the time, *p* is the pressure, ρ is the water density, *g* is the gravity and *C(t)* is a function referred to as the Bernoulli term and is constant for steady flows.

Finally, in accordance with the incident waves, also the spar motions will be described by a sinusoidal function (only in the heave mode, *z* axis, will be analyzed).

Linear theory

All that assumptions will be applied for the formulation of the linear theory that considers the problem of small amplitude water waves.

The boundary conditions are: (a) the bottom of the sea is impermeable; (b) the free surface can be considered as impermeable too assuming that the velocity of the fluid is the velocity on the free surface; (c) the pressure on the free surface is uniform along the wave form (atmospheric pressure).

The solution of the Laplace equation substituting the previous boundary conditions is:

$$\emptyset(x, z, t) = \frac{Hg}{2\omega} \frac{\cosh k(h+z)}{\cosh kh} \cos kx \sin \omega t \tag{3}$$

Where z_1 and z_2 are negative values representing the depths of surfaces A_1 and A_2, respectively.

Moreover, the hyperbolic functions have convenient shallow and deep water asymptotes. Applying the deep water simplifications and defining the cosh *kh* function as:

$$\cosh kh = \frac{e^{kh} + e^{-kh}}{2} \tag{4}$$

The new formulation of the velocity potential for a stationary wave becomes:

$$\emptyset(x, z, t) = \frac{H}{2} e^{kz} \cos kx \sin \omega t \tag{5}$$

Where *H* is the double of the wave amplitude, ω is the angular velocity and *k* is the wave number.

Moreover, the dispersion relationship simplifies for deep water into:

$$\omega^2 = gk \tanh(kh) \cong gk \tag{6}$$

A stationary wave can be decomposed into two progressive waves with the same frequency and amplitude that propagate in opposite directions. The pressure field associated with a progressive wave was determined from the unsteady Bernoulli (Eq. 2) developed for an ideal fluid. For waves of small amplitude, the second order term can be neglected. Therefore, the pressure for a progressive wave is:

$$p = -\rho g z + \rho g \frac{H}{2} \frac{\cosh k(h+z)}{\cosh kh} \cos(kx - \omega t) \tag{7}$$

The interference of the spar in the propagation of the progressive wave can be neglected in a simplified analysis. The Froude-krylov force acts on the body when only the pressure induced for the incident wave is considered. That simplification is reasonable if the body dimension is small compared with the wavelength. The Froude- Krylov term of the excitation force is given by:

$$|F_v| = |F_{v1} - F_{v2}| = \left| \rho g \frac{H}{2} \cos(kx - \omega t)(e^{kz_1} A_1 - e^{kz_2} A_2) \right| \tag{8}$$

Suitable spar geometries should minimize the Froude-Krylov force, [11]. Hence, considering $z_2 = z_1 - L$ and the case of maximum amplitude:

$$|F_v| = \rho g \frac{H}{2} [e^{kz_1}(A_1 - e^{-kL} A_2)] \tag{9}$$

Equation of motion

The equation of motion in time domain according to the Newton second law is given by:

$$\boldsymbol{I}\ddot{\boldsymbol{z}}(t) = \boldsymbol{F_{pe}}(t) + \boldsymbol{F_f}(t) \tag{10}$$

where $\boldsymbol{I}$ represents the inertia matrix, $\ddot{\boldsymbol{z}}$ the acceleration, $\boldsymbol{F_{pe}}$ the force vector due to the external pressure on the buoy and $\boldsymbol{F_f}$ the friction-force vector, which is neglected in accordance with the linear theory assumptions, based on small velocity amplitudes.

All the forces acting on the device will be described by a complex amplitude and sinusoidal time dependence, $e^{i\omega t}$. Hence, the device displacement, velocity and acceleration vectors become respectively:

$$\boldsymbol{z}(t) = Re\{\hat{\boldsymbol{z}}(\omega) e^{i\omega t}\} \tag{11}$$
$$\dot{\boldsymbol{z}}(t) = Re\{i\omega \hat{\boldsymbol{z}}(\omega) e^{i\omega t}\} \tag{12}$$
$$\ddot{\boldsymbol{z}}(t) = Re\{-i\omega^2 \hat{\boldsymbol{z}}(\omega) e^{i\omega t}\} \tag{13}$$

where the hat symbol denotes the complex amplitude.

The force vector $\boldsymbol{F_{pe}}$ may be decomposed into two components to differentiate the sources of static and dynamic pressure. Then,

$$\boldsymbol{F_{pe}} = \boldsymbol{F_{hs}} + \boldsymbol{F_{hd}} \tag{14}$$

where the first term represents the vector of hydrostatic restoring forces due to gravity and buoyancy. This term is proportional to the displacement of the device if no changes in the hydrostatic coefficients matrix, $\boldsymbol{G}$, occurs. In this case, it is given by:

$$\hat{\boldsymbol{F}}_{\boldsymbol{hs}} = -\boldsymbol{G}\hat{z} \tag{15}$$

Where the matrix $\boldsymbol{G}$ of hydrostatic coefficients is for the heave mode element, G_{33}, given by:

$$G_{33} = S\rho g \tag{16}$$

where $S = \pi r_1^2$ is the floating surface.

Furthermore, the second term of Eq. 14 embodies the force vector resultant from the dynamic pressure over the body surface. This term is expressed as:

$$\boldsymbol{F_{hd}} = \boldsymbol{F_e} - \boldsymbol{F_r} \tag{17}$$

The first term of the Eq. 17 corresponds to the excitation force vector and is represented by,

$$\boldsymbol{F_e} = \hat{\boldsymbol{f}}_{\boldsymbol{e}} e^{i\omega t} \tag{18}$$

Where $\hat{\boldsymbol{f}}_{\boldsymbol{e}}$ is the complex amplitude of the excitation force. Furthermore, the second term of Eq. 17 corresponds to the radiation force vector. The radiation force is related to the waves produced by the body motions. It comprises two terms, one related to the velocity and another to the acceleration. Therefore, it results from:

$$\hat{\boldsymbol{F}}_{\boldsymbol{r}} = i\omega\boldsymbol{B}\,\hat{z} - \omega^2\boldsymbol{M}\hat{z} \tag{19}$$

Here, $\boldsymbol{M}$ and $\boldsymbol{B}$ represent, respectively, the symmetrical matrices of added mass and damping coefficients. The added mass coefficient corresponds to an inertial increment due to the water displaced in the body vicinity when the body moves. The damping coefficient is related with the energy transmitted to the fluid by the body oscillations, which gradually moves away from the body. In this case the energy involved is resistive and it is associated with a dissipative effect.

Therefore, taking on account the equations (Eq. 15, 18 and 19):

$$\hat{\boldsymbol{F}}_{\boldsymbol{pe}} = \hat{\boldsymbol{f}}_{\boldsymbol{e}} - i\omega\boldsymbol{B}\hat{z} + \omega^2\boldsymbol{M}\hat{z} - \boldsymbol{G}\hat{z} \tag{20}$$

Which represents the total force acting on a free floating body.

Substituting Eq. 20 into Eq. 10 and using Eq. 11, 12 and 13, the final equation of motion is:

$$\hat{\boldsymbol{z}} = \frac{\hat{\boldsymbol{f}}_{\boldsymbol{e}}}{(-\omega^2(m + \boldsymbol{M}) + \boldsymbol{G}) + i\omega\boldsymbol{B}} \tag{21}$$

Where m is the mass of the SPAR calculated as the mass of displaced water in the free floating condition.

RESPONSE OF A VARIABLE GEOMETRY SPAR

Preliminary design

The dimensions of the SPAR affect his stability. The first study is to choose the best dimensions for the cylinders. From equation Eq. 9 one can see that the vertical forces are zero when:

$$r = \frac{A_2}{A_1} = e^{kL} \tag{22}$$

Where r is the area ratio between A_2 and A_1, L is the length of the external cylinder and k is the wave number.

Fig. 2 shows the relation between the area ratio and $k{\cdot}L$ when the vertical forces are zero for a period of 10s. Taking the peak frequency of the spectrum of density for the north Portuguese coast in winter, that has the value of 0,62 rad/s, one can calculate different combinations of dimensions.

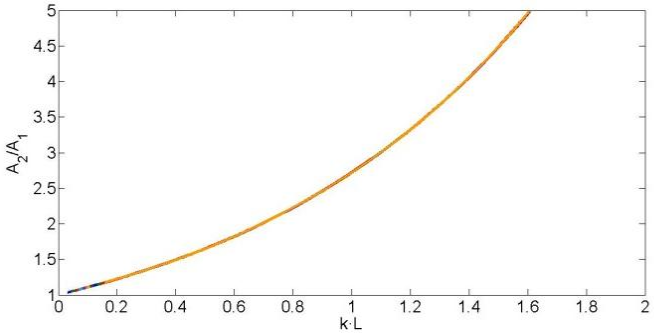

Fig. 2: Area ratio $r = A_2/A_1$ as a function of $k \cdot L$ for $F_v = 0$

Fig. 3 shows the vertical forces acting on the spar for different combination of area ratios as a function of the period. Thus, the one that minimize them is the relation of *r=3,194*.

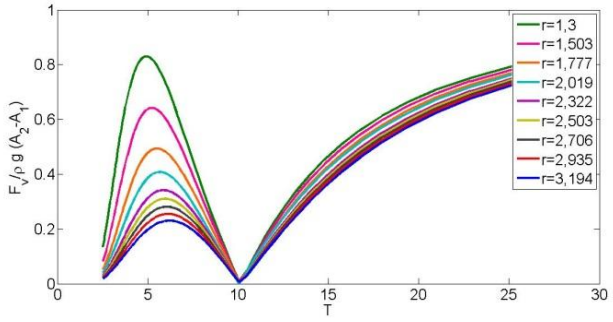

Fig. 3: Dimensionless force as a function of T for different candidate dimensions and for $r_1 = 5m$ and $z_1 = -5$.

Imposing $r_1=5m$ and $z_1=-5m$, the rest of the dimensions are calculated for the area ratio chosen, *r=3,194*, before obtaining the spar shown in Fig. 4:

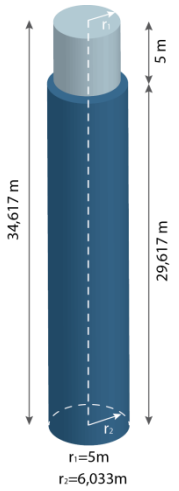

Fig. 4: Spar with the final dimensions.

Vertical motions study

The vertical response of the spar with the final dimensions is shown in Fig. 5. Between 0,4 and 0,45 the displacement is extremely high because the spar resonance frequency is within this frequencies range. However, the displacements at that particular frequencies range will be high due to the resonance, but much lower than the values computed.

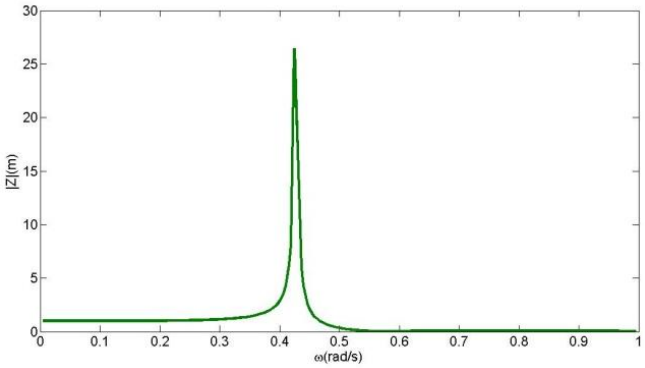

Fig. 5: Spar vertical displacement as a function of ω for the selected dimensions.

The resonance frequency is calculated as:

$$\omega_r = \sqrt{\frac{G}{m+M}} \tag{23}$$

Therefore, adding mass decrease the resonance frequency. The addition of an inertial plate at the bottom of the spar produces that effect. Moreover, changing the porosity of the plate the dynamic response of the spar may be significantly affected, which may be useful to reduce the body vertical motion within the most common frequencies range. As the software used to calculate the G and M coefficients isn't able to work with the porosity variable, the solution adopted was to simulate a variation of the radius of the plate, r_p, as Table 1 shows:

Table 1. Porosity variation (%) for each plate radius r_p.

% Porosity	r_p (m)
60%	7
47%	8
33%	9
18%	10
0%	11

The response of the spar with the inertial plate is shown in Fig. 6. Varying the porosity between 0 and 60% the interval of high vertical motions goes from 0,32 and 0,45 rad/s. In that interval, the response of the body is not simulated, as the results are unrealistic due to the limitations of the linear theory, as explained in the previous section. Furthermore, as the porosity of the plate increases the bandwidth of high motions becomes narrow and is displaced to low frequencies (both facts are consequence of the inertia augment due to the added mass increase).

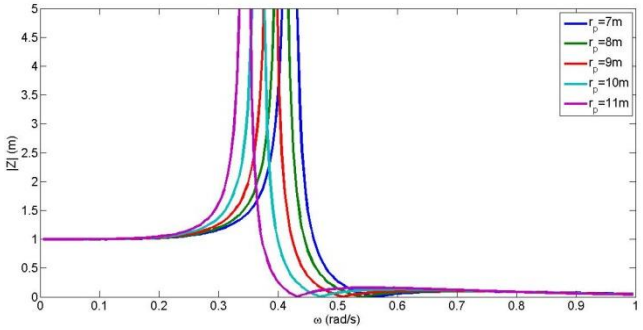

Fig. 6: Vertical motion amplitudes as a function of ω for several radius of the plate considered.

The augment of the added mass coefficient M provokes that the resonance frequency decreases. The resonance frequency may be also reduced by decreasing the radius of the inner cylinder r_1 (small hydrostatic coefficient). Choosing a variation of the radio, r, until 50%, the different radiuses obtained are summarized in table 2.

Table 2. % Area ratio variation and its corresponding r_1.

% r variation	r_1
-50 %	3,7
-44 %	4
-25 %	4,6
0 %	5
25 %	5,2
50 %	5,4

When the area ratio, r, is increased the radius r_1 decreases and, for that reason, the mass of the structure decrease, too. However, the curves in Fig. 7 show, as expected, that the resonance frequency decreases when the radius r_1 is reduced. Thus, the variation of the hydrostatic coefficient G is more important, than the effect of the mass reduction, to change the resonance frequency. Playing with a contraction or expansion of the inner cylinder the dynamic response of the spar may be significantly affected as Fig. 7 shows.

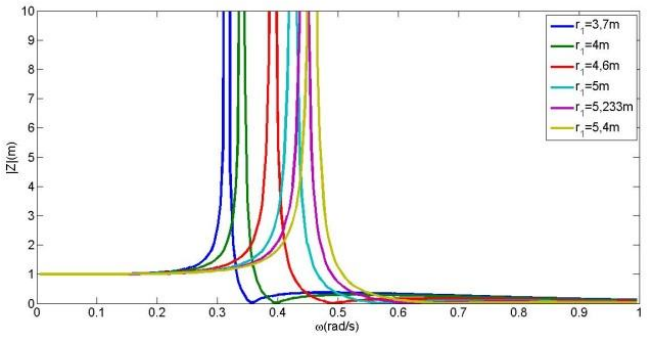

Fig. 7: Vertical motion amplitudes as a function of ω with a variation of r until 50 %.

CANDIDATE SOLUTIONS TO CHANGE THE SPAR GEOMETRY

The materials for offshore structures should be resistant to the corrosion of the seawater which is the property that causes most problems. Moreover, the candidate material for the damping plate, according to the results obtained before, should be able to vary his porosity.

Nowadays, the most common materials for offshore structures and production applications are (a) Carbon and low alloy steels used for structures and pipelines and production/process equipment; (b) Corrosion resistance alloys used for production and process equipment's that are subjected to corrosive environments containing CO_2 and H_2S. They involve stainless steels, nickel base alloys, cobalt base alloys, nickel-copper alloys and titanium alloys; (c) Non-metals including elastomers, coatings, plastics and composites, [4].

For the study only options (a) and (c) are valid. The most important problem of the steel is the corrosion and the solutions used nowadays against it are the metallic or organic coatings such as chlorinated rubbers, epoxies and solvent-soluble vinyl resins and the cathodic protection.

Cathodic protection prevents corrosion by converting all of the anodic (active) sites on the metal surface to cathodic (passive) sites by supplying electrical current (or free electrons) from an alternate source. Magnesium, aluminum and zinc alloys are the most frequently used sacrificial anode systems.

From option (c), composites offer interesting properties to substitute steel applications but they are still in development for offshore structures of wind plants. These properties are:

- Low maintenance: Concrete is a durable material that can keep his properties under extreme conditions and it is not affected as steel with corrosion problems.
- Design and construction flexibility
- Concrete solutions are fully recyclables.
- Concrete can provide long life solutions capable of accommodating to future wind turbines models.

The porosity variation in the case of concrete is function of the temperature: as the temperature increase the % of porosity augments too. Nonetheless, when the porosity increases the strength and ductility decrease which is not a requirement of the spar. For this reason, the concrete is discarded as a possible candidate for the damping plate. Moreover, increasing the temperature of the material in an offshore application to control just the porosity is a waste of energy in turn that other important properties of the materials are damaged.

The next option is try to find a smart material able to change the porosity and with the strength and corrosion requirements for an offshore application. Nowadays, the porosity of some materials can be controlled when they are manufactured. This control is at microscopic level. The damping plate needs a variation of the porosity from 0% until 60%. With 0% of porosity the material will be ductile and on the other hand, with 60% of porosity will be fragile. Therefore, the increase of porosity of the material detriment the ductility property and the resistance so there is not any existent material with the requirements specified.

The proposed solution consists in a mechanical plate with holes that simulate the voids of the material but in a macroscopic scale. The mechanism will have two parts: one fixed and another mobile, composed like a "sandwich". The mobile part is a plate with 72 holes with a radius of 60cm distributed like is shown in Fig. 8.

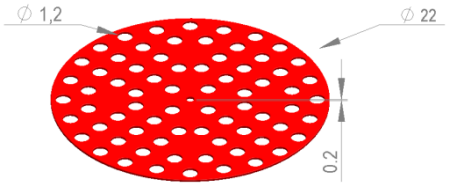

Fig. 8: Mobile part of the damping plate with 72 holes of r_h= *0,6m* Dimensions in meters.

The fix part of the design has two equidistant and concentric plates with the same number of holes and distribution of the mobile one and is fixed to the bottom of the external cylinder.

The proposed material for the mechanical damping plate is the 6Mo and 25Cr duplex stainless steel with a barrier coating typified by an inert pigmentation, typically titanium dioxide. The degree of protection offered by the barrier depends on the thickness of the coating system as well as the generic type and nature of the binder system but in general offers good strength and abrasion resistance as well as good resistance towards UV-radiation. The surface should have a cyclic corrosion testing based on standards. In Europe, ISO 12944 is the most accepted test of anticorrosive properties. Fig. 9 shows the proposed design.

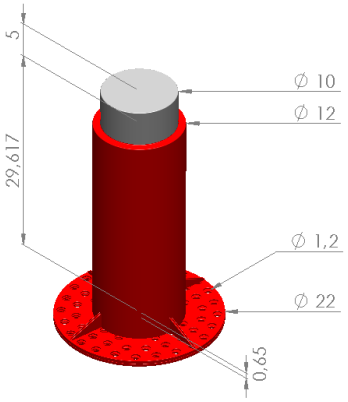

Fig. 9: Final design of the proposed solution with the dimensions in meters.

CONCLUSIONS

The dimensions of the spar are calculated in order to minimize the vertical forces, which are formulated with the linear theory assumptions, fixing some parameters initially like the radius of the inner cylinder, r_1, and its height, z_1. Both variables took as first iteration the value of 5m, in accordance to other solutions already proposed and under development nowadays.

Once the dimensions of the spar were selected, the next step was the analysis of the spar vertical motions. Within the range of frequencies between 0,4 and 0,45 rad/s the spar vertical motions were too high due to resonance. However, the displacement values in that interval are unrealistic because non -linear viscose effects (which play an important rule for high velocities) are not considered in the model (based on linear theory).

For the particular density spectrum considered (which characterize the more common sea state of the north of Portugal) was verified that the high motions bandwidth coincide with the more relevant spectral frequencies. Thus, the bandwidth and the resonance frequency must be modified and the initial hypothesis to do it was the addition of an inertial plate on the bottom of the spar to increase the added mass and decrease the resonance frequency. Varying the porosity of the plate, the resonance frequency of the spar may be modified in order to deviate it from the most relevant frequencies of the sea state. This method reveled to be promising and might be useful to control the dynamics of wind offshore platforms.

On the other hand, the variation of the inner cylinder radius r_1 produces a displacement of the resonance frequency due to the strong effect of the hydrostatic coefficient G. This effect was quantified and seems to be a likely alternative to control the dynamics of the platform.

After the motion study, the problem gets focused to find a material for the inertial plate able to vary his porosity. Nowadays, it doesn't exist any material able to vary that property in the scale required. The proposed solution is a mechanical inertial plate with holes to simulate the porosity variation made of 6Mo and 25Cr duplex stainless steel with a barrier coating of titanium dioxide to protect the spar of seawater corrosion.

The proposed design can be improved in the future making a optimization study that maximize the surface of the holes taking into account that there should be enough area on the plate to cover them and calculate the optimum distribution around the surface.

Finally, the study of motion done in chapter is not realistic for the solution found for the inertial plate due to the simplifications of the linear theory. It is recommended to study the movement of the damping plate taking on account viscosity effects to study the movement of the spar with a model more realistic.

ACKNOWLEDGEMENTS

I would like thank my supervisor, Antonio Sarmento, for making this thesis possible and his collaboration with suggestions and corrections that helped me in my first research experience. I want to thank him too the opportunity that give me to work in the Wave Energy Centre that contributes to my formation and learning very positively.

The calculus of the motion equation haven't been possible without the collaboration of Marco Alves (WaveEC) and Matthieu Guérinos (IST, PhD student) that helped me doing some of the necessary calculus with WAMIT. Miguel Vicente (WaveEC) helped me learning Matlab and solves all my doubts.

I would like to thank the collaboration of the Centre for Nanotechnology and Smart Materials, CeNTI, and especially to João Gomes (CeNTI) and Bruno Matos (CeNTI) giving me the opportunity to stay in their installations working, providing me all the necessary bibliography and helping me to find a solution to my problem.

REFERENCES

[1] BABOIAN, R. Corrosion tests and standars. ASTM International, 2005, ch. Types of Data, pp. 59–64.

[2] BABOIAN, R. Corrosion tests and standars. ASTM International, 2005, ch. Surface analysis, pp. 76–80.

[3] BRITO E MELO, A. Ocean energy: state of the art. Tech. rep., Wave Energy Centre, November 2009.

[4] CHAKRABARTI, S. K. Handbook of Offshore Engineering. Elsevier, 2005, ch. Materials for Offshore Applications, pp. 1127–1137.

[5] FALNES, J. Ocean waves and Oscillating systems. Cambridge University Press, The Edinburd building, Cambrigde CB2RU, UK, 2002.

[6] J. BOXALL AND J.A. VON FRAUNHOFER. Paint formulation: Principles and Practice. George Godwin Limited, 1980, ch. Formulating of Coating for Steelwork, pp. 91–94.

[7] LOPES, M. Experimental Development of Offshore Wave Energy Converters. Ph.D. Dissertation, Department of Mechanical Engineering, IST, Universidade Técnica de Lisboa, November 2010.

[8] P.A. SØRENSEN, S. KIIL, K. DAM-JOHANSEN AND C.E. WEINELL. Anticorrosive coatings: a review. Tech. rep., Technical University of Denmark, Department of Chemical and Biochemical Engineering, 2008.

[9] R. BAXTER AND J. BRITTON. Offshore cathodic protection 101: What it is and how it works. WWW page, 2011.

[10] R. G. DEAN AND R. A. DALRYMPLE. Water wave mechanics for engineers and scientist. World Scientific, 1991, ch. A review of Hydrodinamics and Vector Analysis, pp. 6–36.

[11] R. G. DEAN AND R. A. DALRYMPLE. Water wave mechanics for engineers and scientist. World Scientific, 1991, ch. Small-Amplitude Water Theory Formulation and Solution, pp. 41-72.

[12] REVE. First offshore floating wind turbine in Portugal. WWW page, January 2011.

[13] ROBERGE, P. R. Handbook of corrosion engineering. WWW page, 2000.